15th INTERNATIONAL MULTIDISCIPLINARY SCIENTIFIC GEOCONFERENCE
S G E M 2 0 1 5

INFORMATICS, GEOINFORMATICS AND REMOTE SENSING
CONFERENCE PROCEEDINGS
VOLUME I

\- -

INFORMATICS, GEOINFORMATICS

PHOTOGRAMMETRY AND REMOTE SENSING

\- -

18-24, June, 2015
Albena, BULGARIA

84. HYBRID GEOPROCESSING WEB SERVICES, Evgeny Panidi, Eduard Kazakov, Evgeny Kapralov, Anton Terekhov, Saint-Petersburg State University, Russia… 669

85. IMPROVING OF TRANSMISSIVITY MAPS FOR HYDROGEOLOGICAL MODEL OF LATVIA, Dr.sc.ing. Aivars Spalvins, Dr.geol. Olgerts Aleksans, Inta Lace, Riga Technical University, Latvia 677

86. INFORMATION-ANALYTICAL SYSTEM OF ENVIRONMENTAL MONITORING, Dr Maxim Medvedev, Ural Federal University, Russia 685

87. INTELLECTUAL GIS TECHNOLOGIES IN HISTORICAL AND ETHNOGRAPHIC RESEARCH, Yan Ivakin, Misha Tsvetkov, Vladislav Ivakin, St. Petersburg Institute for Information and Automation, Russia......................................691

88. INTERACTIVE SYSTEM FOR ENVIRONMENTAL MONITORING OF TRAFFIC JAM, Assoc. Prof. Alexander. V. Ivanov, Assoc. Prof. Alexander Yu. Platov, Graduate student Marina S. Belyakova, Master student Ekaterina A. Kaminskas, Nizhny Novgorod State University of Architecture and Civil Engineering, Russia 699

89. MANAGING RURAL AREAS CONSIDERING CLIMATE CHANGES AND EXTRAORDINARY WEATHER PHENOMENA – A CONCEPT OF SOLUTIONS ON A LOCAL SCALE, Kocur-Bera Katarzyna, Dudzinska Malgorzata, University of Warmia and Mazury, Poland...707

90. MAPPING HEAVY METAL CONTAMINATION BY KRIGING IN VALEA SESEI TAILING POND, ROMANIA, Cornelia Melenti, PhD. Ioana Laura Magyar , Technical University of Cluj-Napoca, Romania 715

91. MERCURY CONTENT AS A PART OF A MULTI-CRITERIA ANALYSIS OF INVESTMENT POTENTIAL OF POST-MINING AREAS, PhD Anna Michalska, PhD Krzysztof Michalski, Central Mining Institute (GIG), Poland 723

92. METHODS FOR EXTERNAL FACTORS ASSESSING WITHIN GEOINFORMATION MANAGEMENT OF TERRITORIES, Prof. DSc. E. P. Istomin, Assoc. Prof DSc. A. G. Sokolov, Assoc. Prof. DSc. V. M. Abramov, Assoc. Prof. DSc. G. G. Gogoberidze, PhD A.A. Fokicheva, Russian State Hydrometeorological University, Russia 729

93. MINERAL AND ANTHROGHENE ACCESS DATABASES ORGANIZATION FOR ALSHAR POLYMETALLIC DEPOSIT AND WASTE DUMP, FYR OF MACEDONIA, M.Sc Dalibor Serafimovski, Prof. Vlado Gicev Prof. Kosta Mitreski , University Goce Delcev, FYR of Macedonia....................................737

94. MODELING OF DECISION SUPPORT SYSTEM FOR SPATIAL PLANNING BASED ON ANFIS MODEL, Assist. Prof. Jasna Pleho, Prof. Zikrija Avdagic, Arch Design d.o.o., Bosnia and Herzegovina 745

IMPROVING OF TRANSMISSIVITY MAPS FOR HYDROGEOLOGICAL MODEL OF LATVIA

Dr.sc.ing. Aivars Spalvins

Dr.geol. Olgerts Aleksans

Mg.sc.ing. Inta Lace

Riga Technical University, **Latvia**

ABSTRACT

In 2010 – 2012, the hydrogeological model (HM) of Latvia (LAMO) has been developed by scientists of Riga Technical University (RTU). LAMO generalizes geological and hydrogeological information accumulated by the Latvian Environment, Geology and Meteorology Centre. The commercial program Groundwater Vistas (GV) was used for running LAMO. In 2013 – 2014, LAMO was considerably upgraded. Density of the hydrographical network (rivers and lakes) was increased, cuttings of river valleys into primary geological strata were accounted for, transmissivity distributions for aquifers were refined. To improve transmissivity data of HM aquifers, information provided by pumping tests for wells was used. The refined transmissivity data were applied to create the permeability maps of aquifers as the variable initial data for the GV system. To accomplish this task, methods of numerical interpolation and digital image processing were used.

Keywords: Hydrogeological model, numerical interpolation, pumping tests for wells, transmissivity of aquifers, hydrographical network.

INTRODUCTION

In 2010 – 2012, HM LAMO was developed and, in 2013 – 2014, it was upgraded by scientists of RTU [1]. Presently, four successive versions of LAMO can be marked (Table 1). LAMO comprises the active groundwater zone that provides drinking water. The location of LAMO is shown in Fig. 1. Most of the geological layers are outcropping and, for this reason, they are not present everywhere in the HM area (see Fig. 2 and Fig. 3). After emerging at the surface, such layers have the zero thickness $m = 0$. To avoid in GV calculations “the division by zero”, $m = 0$ must be replaced by small $\varepsilon > 0$ (for LAMO, $\varepsilon = 0.02$ meter). As it follows from the vertical schematization of HM (Fig. 4), the current version of LAMO3 simulates 27 geological layers.

To comprehend the layer transmissivity effect, basic mathematical expressions of numerical hydrogeological modelling [1] must be considered. Vector φ of the piezometric head is the numerical solution of the boundary field problem which is approximated in nodes of the HM *xyz*–grid by the following algebraic expression:

$$A\varphi = \beta - G\psi, \qquad A = A_{xy} + A_z \tag{1}$$

where A is the symmetric sparse matrix of the geological environment which is presented by the *xy*-layer system containing horizontal (A_{xy} – transmissivity T) and vertical (A_z – vertical hydraulic conductivity) elements of the HM grid; ψ and β are the boundary head and flow vectors, respectively; G is the diagonal matrix (part of A) assembled by elements linking the nodes where φ must be found with the nodes and points where ψ is given.

Fig. 1. Location of LAMO.

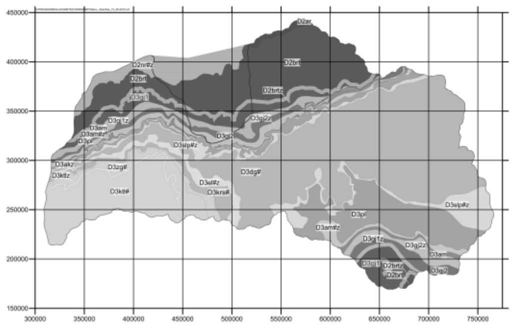

Fig. 2. Boundaries of primary geological strata.

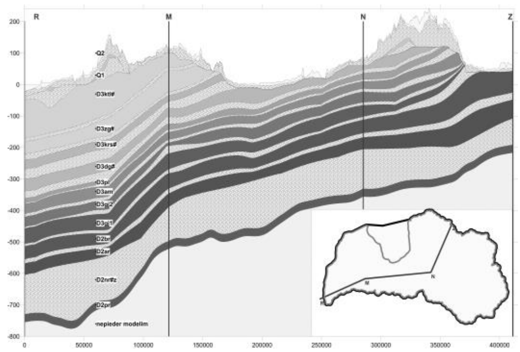

Fig. 3. Geological cross section.

No of HM plane		Name of layer	Geolo-gical code	HM plane code
1.		Relief	relh	relh
2.		Aeration zone	aer	aer
3.		Unconfined Quaternary	Q4-3	Q2
4.		Upper moraine	gQ3	gQ2z
5.		Confined Quaternary or Jura	Q1-3 J	Q1#
6.		Lower moraine or Triass	gQ1-3 T	gQ1#z
7.		Perma Karbons Skerveles Ketleru	P2 C1 D3šķ D3ktl	D3ktl#
8.		Ketleru	D3ktl	D3ktlz
9.		Zagares Svetes Tervetes Muru	D3žg D3sv D3tr D3mr	D3zg#
10.		Akmenes	D3ak	D3akz
11.		Akmenes Kursas Jonisku	D3ak D3krs D3jn	D3krs#
12.		Elejas Amulas	D3el D3aml	D3el#z
13.		Stipinu Katlesu Ogres Daugavas	D3stp D3ktl D3og D3dg	D3dg#
14.		Daugavas Salaspils	D3dg D3slp	D3slp#z
15.		Plavinu	D3pl	D3pl
16.		Plavinu Amatas	D3pl D3am	D3am#z
17.		Amatas	D3am	D3am
18.		Upper Gauja	D3gj2	D3gj2z
19.		Upper Gauja	D3gj2	D3gj2
20.		Lower Gauja	D3gj1	D3gj1z
21.		Lower Gauja	D3gj1	D3gj1
22.		Burtnieku	D2brt	D2brtz
23.		Burtnieku	D2brt	D2brt
24.		Arikula	D2ar	D2arz
25.		Arikula	D2ar	D2ar
26.		Narvas Narvas	D2nr2 D2nr1	D2nr#z
27.		Pernavas	D2prn	D2pr

- aquitard

-united aquifer; #z – united aquitard

Fig. 4. Vertical schematization of LAMO3.

Table 1: Versions of LAMO

Name of version	Year of dispose	Approximation grid			Rivers in model			Lakes
		Plane step [meter]	Number of grid planes	Number of cells [$\times 10^6$]	Number	Valleys incised	Flow data used	Number
LAMO1	2012	500	25	14.25	199	no	no	67
LAMO2	2013	500	27	15.43	199	yes	no	67
LAMO3	2014	500	27	15.43	469	yes	no	127
LAMO4	2015	250	27	61.56	469	yes	yes	127

The transmissivity elements a_{xy}, of A_{xy}, of the HM xy-planes are computed, as follows:

$$a_{xy} = k_i\, m_i = T_i\,, \qquad m_i = z_{i-1} - z_i \geq 0, \qquad i = 1, 2, \ \ldots, u \tag{2}$$

where z_{i-1} and z_i are elevations, accordingly, of the top and bottom surfaces of the i-th geological layer; u - the number of layers (for LAMO3, u = 27); z_0 - ground surface elevation ψ_{rel} map (top of the 1st layer); k_i and m_i - elements of the digital k and m-maps of the i-th layer permeability and of the computed thickness, accordingly. The set of z-maps represents the geometry (stratigraphy) of HM.

The m-maps are obtained from the z-maps and the matrix T_i is also computed within the GV system [2]. For this reason, it is difficult to change the m-maps (HM geometry) and, to control the transmissivity T, one has to apply the variable permeability k-maps.

The transmissivity T for aquifers is very important, because it controls the groundwater motion there. For aquitards a_{xy}~0, because their permeability k is very small. The effect of T is insignificant for aquitards.

The permeability of aquifers can be measured in a variety of ways: field tests, laboratory tests, methods based on grain size distributions [3]. Inverse problem solving methods can also be applied [4]. However, the field tests where one pumping well is used are commonly applied. They permit the testing of large volumes of rock and they provide rather reliable data for finding transmissivity of aquifers. To improve the T-maps of LAMO3, the single well pumping data were applied.

APPLICATION OF PUMPING TEST RESULTS FOR OBTAINING TRANSMISSIVITY DATA

The single well pumping test of the confined aquifer uses the discharge rate Q and the drawdown S of the groundwater head is observed. The test is presented by the expression [5]:

$$S = \frac{Q}{2\pi T}(\ln(R/r) + \xi + \gamma)\,, \qquad T = km \tag{3}$$

where R and r are radiuses, accordingly, of the well depression cone and the screen; ξ and γ are additional hydraulic resistances that account for the partial penetrating factor of a well and for the quality of the well screen, respectively. For a new well, γ=0. For old wells, the screen resistance γ increases. Then the value of γ is unknown and, for this reason, only pumping data of the new wells can provide reliable results and then γ=0 should be used in (3).

From (3), one can obtain:

$$T = \frac{q}{2\pi}(\ln(R/r) + \xi)\,, \qquad q = Q/S \tag{4}$$

where q is the well specific capacity.

If q and T have the dimensions [litre/(sec.meter)] and [(meter)^2/day], respectively, then

$$T = 13.75q(\ln(R/r) + \xi)\,. \tag{5}$$

Primary aquifers of LAMO are leaky and confined. Then $R = 1.12B$ [6]:

$$B = \sqrt{\frac{km}{k_1/m_1 + k_2/m_2}} \tag{6}$$

where B is the leakage factor, $T = km$ - transmissivity of the aquifer, k_1, m_1 and k_2, m_2 are permeability and thickness of the leaky confining aquitards, accordingly, located above and below the aquifer. In Table 2, values of B, R and $ln(R/r)$ are given for a typical aquifer of LAMO when r = (0.05 – 0.1) meter; k [meter/day]; B, R, m [meter].

Table 2. Computed values of B, R, $ln(R/r)$

km	k_1,k_2	m_1,m_2	B	R	r	$ln(R/r)$
200	10^{-4}	10	3162	3542	0.1	10.47
200	10^{-4}	5	2236	2504	0.1	10.12
200	10^{-4}	10	3162	3542	0.05	11.17
200	10^{-4}	5	2236	2504	0.05	10.82

By exploiting the fact that in Table 2 $ln(R/r)$~10.5, one can approximate (5). If $\xi = 0$ then the following formula roughly provides the minimal value T_{min} of transmissivity for the confined aquifer:

$$T_{\min} = 144\, q\,. \tag{7}$$

In [5], the following formula is presented for computing of the resistance ξ:

$$\xi = (1/a - 1)(\ln 1.47ab - 2.65a), \qquad a = l/m, \qquad b = m/r \tag{8}$$

where m is the thickness of an aquifer and l and r are, accordingly, the length and radius of the well screen. The formula can be used if $m/r > 100$, $l/m \geq 0.1$. In Table 3, the results given by (8) are presented.

Table 3. Values of well hydraulic resistance ξ

l/m	m/r			
	100	200	500	1000
0.1	21.80	28.04	36.29	42.53
0.2	11.40	14.18	17.84	20.61
0.3	6.98	8.60	10.73	12.35
0.4	4.52	5.56	6.93	7.98
0.5	2.97	3.66	4.58	5.27
0.6	1.92	2.41	3.00	3.46
0.7	1.19	1.49	1.88	2.17
0.8	0.63	0.83	1.06	1.24
0.9	0.28	0.35	0.46	0.53
1.0	0.00	0.00	0.00	0.00

The resistance ξ can be applied, to refine the transmissivity T, as follows:

$$T = T_{\min}(1 + \xi/10.5) = cT_{\min}\,. \tag{9}$$

For LAMO, the typical values of *l/m* and *m/r* are within the limits: 0.5 > *l/m* > 0.2; 500 > *m/r* > 100. Then, as it follows from Table 3, the correction *c* may be within the limits: 2.8 > *c* > 1.3.

OBTAINING OF PERMEABILITY MAPS

The *k*-maps of permeability must be used to control the *T*-maps of the GV system:

$$k = T/m \tag{10}$$

where the transmissivity *T* is derived from the well pumping data; *m* is the aquifer thickness which is used in (2) by the GV system.

By using the EXCEL program [7], the set of the specific capacity *q* [litre/(sec.meter)] must be extracted from the well pumping data. As a rule, the *q*-set contains improbable very low and also very high values. In order to normalize the set, minimal and maximal values of *q* are fixed (for LAMO3, q_{min} =0.3 and q_{max} =5). The *q*-set contains *n* pointwise data. For LAMO, *n* > 1000 for practically all aquifers. Due to the large *n*, the fast gridding method of “inverse distance to power” is applied by the SURFER program [8]. This method computes the interpolated value σ_o at the grid nodes by using the available pointwise data σ_i = 144 q_i , i = 1,…, *n*, as follows [9]:

$$\sigma_o = (\sum_{i=1}^{n} \sigma_i \tau_i) / \sum_{i=1}^{n} \tau_i \ , \qquad \tau_i = (1/d_{oi})^p, \qquad d_{oi} = \sqrt{(x_o - x_i)^2 + (y_0 - y_i)^2} \tag{11}$$

where τ_i – the weight of σ_i ; d_i – the distance between the grid node *o* and the σ_i point; *p* - the weighting power; x_o, y_o; x_i, y_i are coordinates, respectively, of the *o*-th grid node and the *i*-th point. The value *p* = 2 was used, to prepare the σ-grid for LAMO3.

The interpolation result of (11) was rather rough and, to smooth it, the moving digital “inverse distance” low-pass filter of the size 11×11 (5km×5km area) was used [10]:

$$\sigma_{oo} = (\sum_{i,j} \sigma_{ij} \tau_{ij}) / \sum_{i,j} \tau_{ij} \ , \qquad \tau_{ij} = (1/D_{ij})^p, \qquad D_{ij} = \sqrt{i^2 + j^2} \tag{12}$$

where τ_{ij} – the weight of σ_{ij} ; *p* - the power (*p* = 0.5 was applied); *i* and *j* were the grid row and column local indices for the neighboring nodes with respect to the central node *oo* of the filter; D_{ij} - the distance between the nodes *oo* and *ij*. In Table 4, the first quadrant of the τ_{ij} matrix of the filter (12) is shown. The filter contains four symmetrical quadrants, because negative *i* and *j* indices are also applied.

Table 4. Weights τ_{ij} for the first quadrant of the 11×11 size filter

j							
5	0.444	0.443	0.431	0.414	0.395	0.376	
4	0.500	0.492	0.473	0.447	0.420	0.395	
3	0.577	0.562	0.527	0.485	0.447	0.414	
2	0.707	0.669	0.595	0.527	0.473	0.431	
1	1.000	0.841	0.669	0.562	0.432	0.443	
0	2.000	1.000	0.707	0.577	0.500	0.444	
	0	1	2	3	4	5	*i*

One can conclude from the values of τ_{ij} in Table 4 that smoothing of the filter is moderate in comparison with the corresponding averaging filter where all weights τ_{ij} = 1.0. To preserve the data provided by wells, only one filtering pass was done.

The "inverse distance" interpolation and filtering do not account for discontinuity of aquifers that include the $m = 0$ areas. Therefore, for all nodes of the 601 × 751 size grid of LAMO, values of transmissivity T_{ij} are computed. To obtain the permeability k-map from the T-grid, the formula (10) must be used where the m-map of thickness is the divider. Only at the aquifer $m > 0$ area reasonable k values can appear. The extreme values of k that are caused by the dividers ε = 0.02 have to be replaced by the largest value k_{max} that can be found within the $m > 0$ area. The final k-map is obtained by applying the filter of (12).

FEATURES OF LAMO2 AND LAMO3 PRIMARY AQUIFERS

For LAMO1 and LAMO2, constant values of k were used to compute the T-maps of primary aquifers. For this reason, T was in the direct proportion to the thickness m of an aquifer. For LAMO, the k-map is presented as the following product:

$$k = k_{norm}\, k_{mean}, \qquad k_{norm} = k / k_{mean}\,, \qquad k_{mean} = \sum_{i=1}^{n} k_i / n \qquad (13)$$

where k_{norm} – the normalized k–map; k_{mean} and n - the mean value of k and the number of grid nodes at the $m > 0$ area, accordingly. For LAMO2, k_{norm} =1.0.

In Table 5, the summary on features of the LAMO2 primary aquifers is presented. The aquifers differ in their areas, mean thickneses m_{mean} and values of k. The mean transmissivity $T_{mean} = k\, m_{mean}$.

Table 5. Summary on features of LAMO2 primary aquifers

Aquifer code	Area [thous.km^2]	m_{mean} [meter]	T_{mean} [meter^2/day]	m_{max}/m_{min} $=T_{max}/T_{min}$	k [meter/day]	k_{max}/k_{min}
D3ktl#	5.44	62.89	188.67	7772.5	3.0	1.00
D3zg#	7.53	50.43	151.29	4382.0	3.0	1.00
D3krs#	9.34	22.71	45.42	2253.0	2.0	1.00
D3dg#	32.84	30.76	307.60	4437.5	10.0	1.00
D3pl	44.10	22.98	229.80	2840.5	10.0	1.00
D3am	46.52	22.11	221.10	2269.0	10.0	1.00
D3gj2	51.17	26.55	265.50	2924.0	10.0	1.00
D3gj1	56.66	31.79	445.06	4287.5	14.0	1.00
D2brt	68.96	45.30	226.50	5520.5	5.0	1.00
D2ar	68.96	41.00	205.00	4904.0	5.0	1.00

Table 6. Summary on features of LAMO3 primary aquifers

Aquifer code	T_{mean} [meter^2/day]	T_{max} $/T_{min}$	k_{mean} [meter/day]	k_{min} [meter/day]	k_{max} [meter/day]	k_{max} $/k_{min}$	$(l/m)_{mean}$
D3ktl#	82.66	2675.0	2.12	0.50	4.50	9.00	0.15
D3zg#	125.38	2062.5	3.64	1.50	8.00	5.33	0.24
D3krs#	121.17	1315.0	5.95	2.30	10.00	4.35	0.36
D3dg#	127.82	2370.0	5.58	0.70	10.00	14.38	0.34
D3pl	156.11	1158.0	6.11	1.78	15.15	8.51	0.55
D3am	94.87	1247.0	4.69	1.50	8.50	5.67	0.53
D3gj2	136.00	1410.0	5.58	2.20	10.00	4.55	0.49
D3gj1	145.62	1220.0	5.24	1.60	10.00	6.25	0.51
D2brt	79.03	1843.0	1.91	0.60	3.50	5.83	0.40
D2ar	80.64	1662.5	2.13	0.65	4.00	6.15	0.50

In Table 6, the main features of the LAMO3 primary aquifers are summarized. Their k-maps are variable (k_{max} $/k_{min}$ >1). Minimal values of T are presented, because the resistances ξ are not accounted for. The mean value of $(l/m)_{mean}$ are given for each aquifer. These values are smaller for the united aquifers D3ktl#, D3zg#, D3krs#, D3dg#. It follows from Table 3 that the correction c of (9) for these aquifers may be within the limits ($2.7>c>1.8$). For the other aquifers, c~1.5.

It follows from the comparison of Table 5 with Table 6 that the k_{mean} and T_{mean} values of the six deeper aquifers D3pl, D2gj2, D3gj1, D2brt, D2ar are considerably smaller for LAMO3. This feature resulted in decrease of groundwater flows there [1]. However, the ratio T_{max}/T_{min} is much larger for LAMO2, because there the ratio depends only on the m-maps.

In the next LAMO4 version, the research on improving the T-maps will continue. The effect of the resistance ξ must be accounted for individual wells, the initial data must checked, in order to exclude the faulty ones. The method that accounts for the m=0 areas have to be improved.

IV. CONCLUSION

Formerly, the constant values represented the permeability k-maps of the LAMO1 and LAMO2 versions. By using the well pumping data, the upgraded variable k-maps have been created. To obtain them, the digital interpolation and image processing methods were applied. Currently, the new k-maps are used in LAMO3 that results in refined transmissivity distributions of the HM primary aquifers. To improve these results, the well geometrical data will be more accurately accounted for and the initial pumping data will be checked and corrected when the next LAMO4 version will be developed.

ATCKNOWLEDGEMENTS

In 2010 – 2012, the hydrogeological model of Latvia LAMO1 has been developed within the framework of the RTU project that was co-financed by the European Regional Development Fund. Upgrading of the LAMO3 and LAMO4 versions are supported by the Latvian State Research Program EVIDEnT.

REFERENCES

[1] Spalvins, A., J. Slangens, I. Lace, K. Krauklis, V. Skibelis, O. Aleksans, and I. Eglite, “Hydrogeological model of Latvia after increasing density of its hydrographical network,” Scientific Journal of Riga Technical University, Boundary Field Problems and Computer Simulation, vol. 53, pp. 12-24, 2014, Available http://www.emc.rtu.lv

[2] Environmental Simulations, Inc., ”Groundwater Vistas. Version 6, Guide to using,” 2011.

[3] Domenico, P. A. and F.W. Schwartz. Physical and Chemical Hydrogeology., John Wiley and sons, Inc. – 2 end ed. 1998, New York, p. 506.

[4] Chin Y.C.. Application of differential evolutionary optimization methodology for parameter structure identification in groundwater modelling. Hydrogeology Journal, Volume 22, Number 8, December 2014, pp. 1731-1748.

[5] Verigin N., Methods Used for Finding Permeability of Geological Strata. Moscow: Gosstroiizdat, 1962 (in Russian).

[6] Bindeman N., and I. Jazvin, Evaluation of Groundwater Resources. Moscow: Nedra, 1982 (in Russian).

[7] Walkenback J., Excel-7 Bible. Indianapolis, Wiley Publishing, Inc., 2007.

[8] Golden Software, Inc., “SURFER-11 for Windows, Users manual, Guide to Using,” 2012.

[9] Franke R., “Scattered Data Interpolation: Test of Some Methods,” Mathematics of Computations, vol.33, pp. 181-200, 1982.

[10] Ditas I., Digital Image Processing Algorithms and Applications, New York: John Wiley and Sons, 2000.